Nonlinear Dynamics of a Controlled Two-wheeled Trailer

Hanna Zsofia Horvath[1], Adam Balint Feher[1], and Denes Takacs[1,2]

[1] Budapest University of Technology and Economics, Faculty of Mechanical Engineering, Department of Applied Mechanics, Budapest, Hungary
hanna.horvath@mm.bme.hu
[2] HUN-REN–BME Dynamics of Machines Research Group, Budapest, Hungary

Abstract. The nonlinear dynamics of towed two-wheeled trailers is investigated using a spatial, 4-DoF model. Namely, the yaw, pitch, and roll motions are all taken into account. Geometrical nonlinearities and the non-smooth characteristics of the tire forces are considered. A linear state feedback controller with feedback delay is designed to enhance the stability performance of the trailer. Numerical bifurcation analysis is performed to investigate the large amplitude vibrations and unsafe (bistable) zones, where the stable rectilinear motion and the stable limit cycle coexist with each other. The effects of the control gain and the feedback delay of the controller are presented on bifurcation diagrams. It is shown, that with appropriately chosen control gains, the size of the bistable region can be limited.

Keywords: towed two-wheeled trailer, stability control, nonlinear analysis, feedback delay

1 Introduction

Vehicle handling and stability are critical factors in road transportation; hence, they became relevant research topics a long time ago, see e.g. [1], [2], [3] and [4]. Unfortunately, several road accidents happen due to the not appropriately chosen amount of payload or payload position, which easily leads to the so-called snaking and rocking motions of trailers. Most of the previous studies are limited to linear stability analysis and are based on single-track (in-plane) models. In this study, we focus on the nonlinear dynamics of two-wheeled trailers, using a spatial mechanical model.

2 Mechanical Model and Control Design

The applied spatial, 4-DoF mechanical model is shown in Fig. 1(a). The trailer is towed with constant towing speed v. For the sake of simplicity, the towing car is imitated by a lateral spring and damper at the kingpin A. The motion of the system can be described with the yaw angle ψ, the pitch angle ϑ, the roll angle φ, and the lateral displacement of the king pin u. Details of the derivation of the governing equations can be found in [5]. Here, we only present the different sources of the relevant nonlinearities and non-smoothness.

Figure 1(b) shows the non-smooth characteristics of the suspension forces. A piecewise smooth formula is introduced for the right $F_{\mathrm{R}} = F_{\mathrm{s}}(d_{\mathrm{R}})$ and the left $F_{\mathrm{L}} = F_{\mathrm{s}}(d_{\mathrm{L}})$ suspension forces, where d_{R} is the distance measured between the points R and R′, and d_{L} is the distance measured between points L and L′, see panel (a) of Fig. 1. We take into account that the right or left tire can detach from the ground, and the related vertical load N_{R} or N_{L} becomes zero. We neglect the effect of the unsprung mass by considering zero masses for the wheels. Hence, zero normal load corresponds to zero suspension forces in our model. In Fig. 1(b), $L_{\max}$ relates to the maximal length of the suspension, i.e., where the suspension is fully expanded. In addition, for $d < L_{\min}$, we consider higher stiffness and damping for the full compression case.

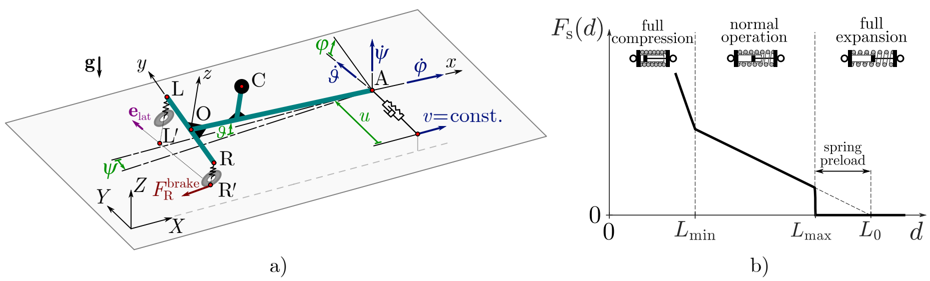

Fig. 1. (a) The towed two-wheeled trailer with the braking force at the right wheel, (b) the schematic non-smooth characteristic of the suspension forces

The effect of the tires is taken into account by means of the lateral tire forces only, which are calculated based on Pacejka's Magic Formula [6]:

$$\mu(\alpha) = D \sin\left(C \arctan\left(B\alpha - E\left(B\alpha - \arctan(B\alpha)\right)\right)\right) , \tag{1}$$

where B, C, D and E are semi-empirical factors, and α is the side slip angle of the right (α_{R}) and the left (α_{L}) wheel. With these, the tire forces are

$$F_{\mathrm{R}}^{\mathrm{tire}} = N_{\mathrm{R}}\,\mu(\alpha_{\mathrm{R}})\,, \qquad F_{\mathrm{L}}^{\mathrm{tire}} = N_{\mathrm{L}}\,\mu(\alpha_{\mathrm{L}})\,. \tag{2}$$

Namely, we assume that the lateral tire forces depend linearly on the vertical loads. In addition, we neglect the dependencies of the factors of the Magic Formula on the static and dynamic coefficients of friction, the temperature, and the camber angle.

To control the snaking motion of the trailer, we design a linear state feedback controller, which operates with the braking forces applied to the right and the left wheels, see Fig. 1(a). We consider braking forces proportional to the yaw rate $\dot{\psi}$ and take into account the deadzone $2\dot{\psi}_0$ of the controller, where no braking force is actuated. Furthermore, we consider the feedback delay τ of the controller. Thus, the non-smooth characteristics of the right and left braking forces can be formulated as

$$F_{\mathrm{R}}^{\mathrm{brake}} = \begin{cases} D(\dot{\psi}(t-\tau) - \dot{\psi}_0)\,, & \text{if} \quad \dot{\psi}(t-\tau) > \dot{\psi}_0\,, \\ 0\,, & \text{if} \quad \dot{\psi}(t-\tau) < \dot{\psi}_0\,, \end{cases} \tag{3}$$

$$F_{\mathrm{L}}^{\mathrm{brake}} = \begin{cases} -D(\dot{\psi}(t-\tau) + \dot{\psi}_0)\,, & \text{if} \quad \dot{\psi}(t-\tau) < -\dot{\psi}_0\,, \\ 0\,, & \text{if} \quad \dot{\psi}(t-\tau) > -\dot{\psi}_0\,, \end{cases} \tag{4}$$

where D is the control gain. The non-smooth characteristics of the tire forces and the braking forces are handled by a smoothed Heaviside-function in our numerical investigation, see, e.g. [5]. Since we investigate the straight running of the two-wheeled trailer, the reference yaw rate is set to zero in this study.

For the sake of simplicity, we do not implement the combined slip in the model. However, we pay attention to the relation between the longitudinal forces (i.e., the braking forces), the lateral tire forces, and the vertical loads. Namely, we define the required coefficients of friction $\mu_{\mathrm{req,R}}$ and $\mu_{\mathrm{req,L}}$ as

$$\mu_{\mathrm{req,R}} = \frac{\sqrt{\left(F_{\mathrm{R}}^{\mathrm{brake}}\right)^2 + \left(F_{\mathrm{R}}^{\mathrm{tire}}\right)^2}}{N_{\mathrm{R}}}\,, \qquad \mu_{\mathrm{req,L}} = \frac{\sqrt{\left(F_{\mathrm{L}}^{\mathrm{brake}}\right)^2 + \left(F_{\mathrm{L}}^{\mathrm{tire}}\right)^2}}{N_{\mathrm{L}}}\,. \tag{5}$$

3 Nonlinear Stability Analysis

Nonlinear bifurcation analysis is carried out with *DDE-BIFTOOL* [7]. The stable and unstable periodic solutions are depicted in bifurcation diagrams, in the plane of the towing speed v and the maximum amplitudes of the yaw angle ψ, the pitch angle ϑ, the roll angle φ, and the lateral displacement of the king pin u, see Fig. 2. Based on the continuation, one can observe that the pitch motion is asymmetric. Thus, both the max/min values of the periodic solutions are illustrated for ϑ. The results are shown for parameter values described in [5], but for vertical payload position of $h = 0.27\,\mathrm{m}$. The half-width of the deadzone was $\dot{\psi}_0 = 0.1\,\mathrm{rad/s}$ in this study.

In the bifurcation diagrams, dashed red lines and solid blue lines refer to unstable and stable motions, respectively. For every branch point of the periodic solutions, the required coefficients of friction of Eq. (5) are calculated. During the continuation of the bifurcation branch, if $\mu_{\mathrm{req,R}}$ and/or $\mu_{\mathrm{req,L}}$ reaches the pre-defined threshold $\mu_{\mathrm{cr}} = 1$, we define the corresponding branch point as the limit of validity. The remaining segment of the bifurcation branch is plotted thin and gray, namely, we consider it invalid.

The bifurcation diagrams in Fig. 2 are constructed for the delay-free case (i.e., $\tau = 0$) for different control gains. For the uncontrolled case (i.e., $D = 0$), a relatively wide bistable region is present, where the stable rectilinear motion coexists with unstable and stable periodic solutions. It is considered an unsafe zone since the global stability of the rectilinear motion is not ensured in this linearly stable towing speed range, and large enough perturbations may lead to unwanted large amplitude vibrations of the trailer. By increasing the control gain, the width of the unsafe zone and the amplitudes of the vibrations are decreased.

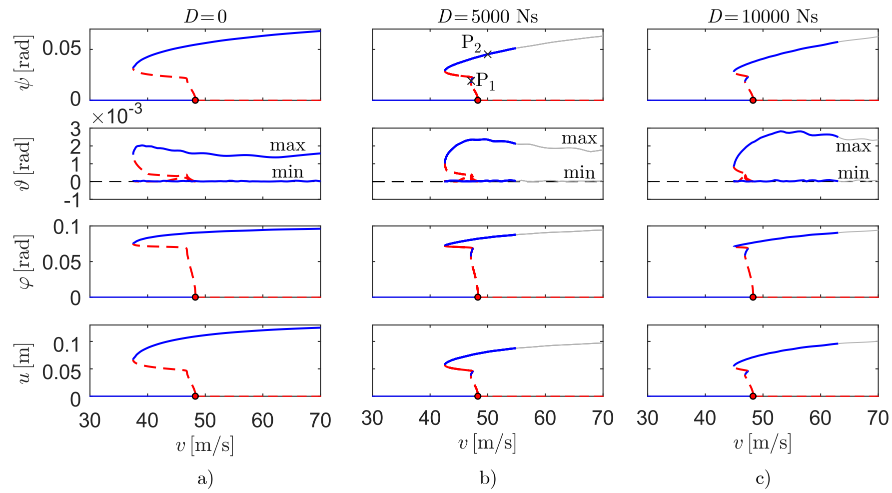

Fig. 2. Bifurcation diagrams with respect to the towing speed v for the delay-free controller ($\tau = 0$) and for different control gains: a) $D = 0$, b) $D = 5000\,\mathrm{Ns}$, c) $D = 10000\,\mathrm{Ns}$

In Fig. 3, numerical results are presented for points P_1 and P_2 of Fig. 2(b). Namely, the periodic solutions for the normal loads, the tire forces, the braking forces, and three of the generalized coordinates (ψ, φ, and u) are plotted for one period T of the oscillation. Point P_1 corresponds to the point of the stable branch with smaller amplitudes and towing speed of $v = 47.22\,\mathrm{m/s}$. As can be observed in Fig. 3(a), no loss of contact of tires happens for this point, i.e., no rocking motion occurs. In addition, the tire forces, the braking forces, and the amplitudes of the vibrations remain moderate. Point P_2 corresponds to the point of the stable branch with larger amplitudes and towing speed of $v = 50.35\,\mathrm{m/s}$. Both full compression and full expansion of the wheel suspension happen, and loss of contact of tires also occurs, see Fig. 3(b). Furthermore, the tire forces, the braking forces, and the amplitudes of the vibrations are remarkably larger.

The effect of the feedback delay τ is shown in the bifurcation diagrams of Fig. 4 for a fixed value of the control gain $D = 5000\,\mathrm{Ns}$. As shown, it significantly affects the nonlinear stability properties. The unsafe zone is narrower, and the amplitudes of the corresponding periodic solutions are smaller for larger feedback delay values. This is a counterintuitive result since it suggests that the feedback delay can be beneficial. Of course, a very large delay (i.e., $\tau \geq 0.2\,\mathrm{s}$) degrades the performance of the controller.

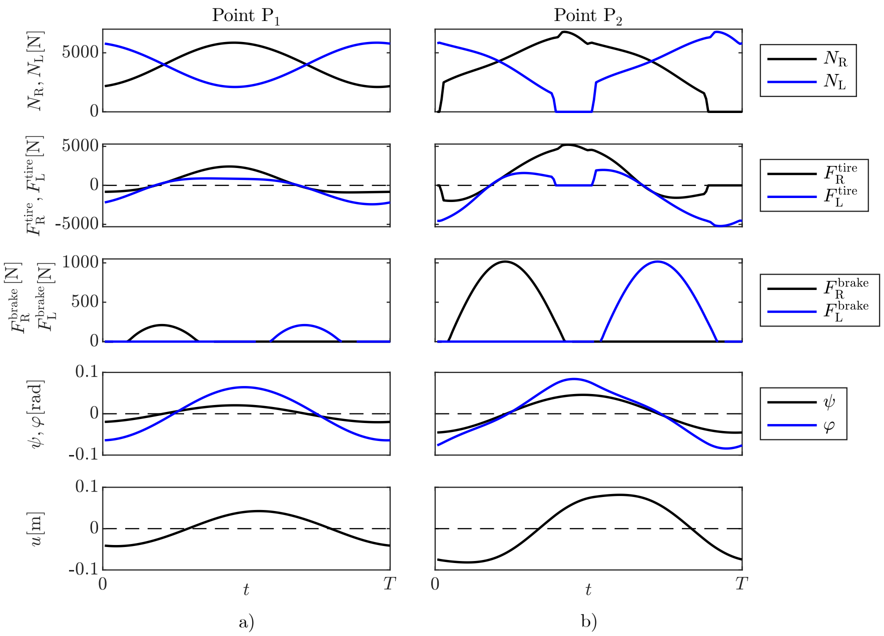

Fig. 3. Numerically determined time histories of the normal loads, the tire forces, the braking forces and the generalized coordinates ψ, φ, and u, for control gain $D = 5000$ Ns and feedback delay $\tau = 0$. Panels refer to the points marked in Fig. 2(b).

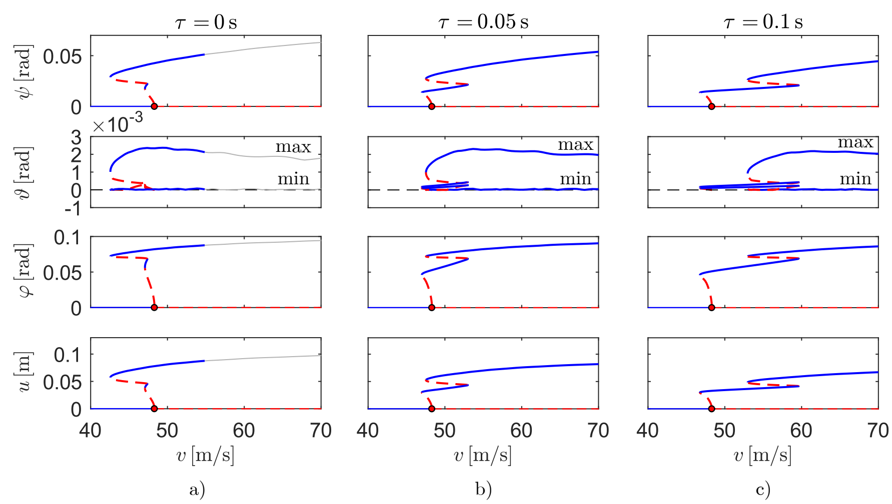

Fig. 4. Bifurcation diagrams with respect to the towing speed v for fixed control gain ($D = 5000$ Ns) and for different feedback delays: a) $\tau = 0$, b) $\tau = 0.05$ s, c) $\tau = 0.1$ s

4 Conclusions

In this study, we performed nonlinear stability analysis of the spatial mechanical model of towed two-wheeled trailers. A linear state feedback controller with feedback delay was designed to reduce the unwanted vibrations of snaking trailers. The deadzone and the feedback delay of the controller were taken into account. For the uncontrolled case, a considerably wide unsafe zone (a so-called bistable region) can be observed. It was shown that this unsafe zone can be reduced by applying braking forces to the wheels. In addition, some feedback delays may have some beneficial effects on global stability.

Acknowledgements

The research is supported by the National Research, Development and Innovation Office under grant no. NKFI-146201, 2020-1.2.4-TET-IPARI-2021-00012 and partly supported by the Janos Bolyai Research Scholarship of the Hungarian Academy of Sciences. Supported by the UNKP-23-5-BME-299, UNKP-23-3-II-BME-137 New National Excellence Program of the Ministry for Innovation and Technology from the source of the National Research, Development and Innovation Fund. This project has received funding from the HUN-REN Hungarian Research Network. The research is partly supported by the Foundation for Mechanical Engineering Education.

References

1. Darling, J., Tilley, D., Gao, B.: An experimental investigation of car-trailer high-speed stability. In: Proc. Instit. Mech. Eng. Part D J. Autom. Eng. **223**(4), 471–484 (2009). https://doi.org/10.1243/09544070JAUTO981
2. Sharp, R. S., Fernandez, M.A.A.: Car-caravan snaking - part 1: the influence of pintle pin friction. In: Proc. Institut. Mech. Eng. Part C J. Mech. Eng. Sci. **216**(7), 707—722 (2002). https://doi.org/10.1243/09544060260128760
3. Troger, H., Zeman, K.: A nonlinear-analysis of the generic types of loss of stability of the steady-state motion of a tractor-semitrailer. Vehicle Syst. Dyn. **13**(4), 161–172 (1984). https://doi.org/10.1080/00423118408968773
4. Kang, X., Deng, W.: Parametric study on vehicle-trailer dynamics for stability control. SAE Technical Paper Series (2003). https://doi.org/10.4271/2003-01-1321
5. Horvath, H. Z., Takacs, D.: Stability and local bifurcation analyses of two-wheeled trailers considering the nonlinear coupling between lateral and vertical motions. Nonlinear Dynamics **107**, 2115–2132 (2022). https://doi.org/10.1007/s11071-021-07120-9
6. Pacejka, H. B.: Tyre and Vehicle Dynamics. Elsevier Butterworth-Heinemann (2002).
7. Engelborghs, K., Luzyanina, T., Samaey, G.: DDE-BIFTOOL v. 2.00: a Matlab package for bifurcation analysis of delay differential equations. Department of Computer Science, K.U.Leuven (2001)